

Variation of the point spread function in the Sargasso Sea

Kenneth J. Voss
University of Miami, Department of Physics
Coral Gables, Fl, 33124

Abstract

Measurements of the Point Spread Function (PSF) were made in the Sargasso Sea in December, 1989. The water column during this period was extremely homogeneous therefore this data set became an obvious candidate to test the theories of Wells¹. This paper describes the results of this study. We show that the formalism (hence the implicit small angle approximation) works reasonably well for this case, with an average difference of 12% between the measured and predicted PSF's.

Theory

The best definition of the PSF is given by Mertens and Replogle.² In this paper they define the $PSF(\theta, \phi, R)$ as the apparent radiance of an unresolved Lambertian source at the position $(0,0,0)$, normalized to source intensity; this quantity has units of m^{-2} . θ is the axial angle between the source, receiver and radiance direction, ϕ is the azimuthal angle and R is the range between the source and receiver. If there was no scattering the PSF would be a delta function. In the ocean, because of forward scattering, the PSF is a rapidly decreasing function centered at $(0,0,R)$. Honey³ has shown that the beam spread function (BSF), the spreading of a light beam due to scattering, is mathematically equivalent to the PSF by reciprocity.

The PSF can be linked to the scattering function for the case of unpolarized light in the small angle limit.¹ In this derivation the $PSF(\theta, \phi, R)$ is the 2 dimensional Fourier transform of the MTF or, since the PSF is rotationally symmetric ($PSF(\theta, \phi, R)$ is independent of ϕ), $PSF(\theta, R)$ is the Hankel (or Fourier-Bessel) transform of the MTF. The MTF is related to a range independent function $D(\omega)$ by:

$$MTF(\omega, R) = \exp(-D(\omega)R). \quad (1)$$

Once the $D(\omega)$ is known for a specific water type, then one should be able to determine the PSF for any arbitrary range. Also the total PSF can be determined for ranges for which individual segments of the PSF have been measured.

To append segments of the PSF to form the total path PSF, the PSF segments must be convolved. By the convolution theorem⁴ and the fact that the MTF is the transform of the PSF, this total PSF can be obtained by multiplying the respective MTF's and then transforming to obtain the final PSF. Mathematically this can be described by:

$$\begin{aligned} \text{if} \quad & R_1 + R_2 = R_3 \\ \text{and} \quad & H\{PSF(R_1, \theta)\} = MTF(R_1, \omega) \\ & H\{PSF(R_2, \theta)\} = MTF(R_2, \omega) \\ \text{then} \quad & H\{MTF(R_1, \omega) MTF(R_2, \omega)\} = PSF(R_1 + R_2, \theta), \end{aligned} \quad (2)$$

where $H\{g\}$ is the Hankel transform of the function g , and R_1, R_2 are the range segments. In the case of a homogeneous water column:

$$MTF(R_1, \omega)^{(1/R_1)} = MTF(R_2, \omega)^{(1/R_2)}. \quad (3)$$

Hence in this case:

$$MTF(R_2, \omega) = MTF(R_1, \omega)^{(R_2/R_1)} \quad (4)$$

Equation 4 implies that the logarithm of the MTF can be reduced to a single range independent portion, the D of the theoretical formalism. It is this dependence that was tested in the experiment.

Instrumentation

To review the instrumentation used in the measurements: the method used to measure the PSF (developed by Honey3) involves a point source (a flashlamp) and a camera system.⁵ The camera system is based on a CCD (charge coupled device) camera and controller made by Photometrics, Ltd. The CCD array (Thompson CSF) is thermoelectrically cooled to allow the array to have very low noise rates (on the order of 10 thermally generated electrons per pixel). The array also has very deep electron wells (can contain 6×10^5 electrons per pixel) allowing a large dynamic range. The CCD is read using a 14 bit A-to-D converter, which takes advantage of the intrinsic dynamic range of the camera.

For this experiment we used two light sources, a 15 Joule and 800 Joule flashlamp.⁶ Each flashlamp had a cosine diffuser to produce a lambertian source, however the smaller source had a much more accurate distribution; within 5% of the exact cosine distribution. The instruments were used in two configurations, the first is with the camera remaining just below the surface of the water and varying the depth of the light source. In this method the variation of the PSF with R is investigated. The second configuration placed the camera and light source a fixed distance apart and varies the overall depth of the system. In this way the system is used to profile the PSF through the water column.

Data Processing

The cast selected to test these theories had very homogeneous optical properties from the surface to 80 m. The beam attenuation varied from 0.082 to 0.074 m^{-1} over this range (measurement in the blue-green). Further evidence of the homogeneity of the water column was given by the measurements of the PSF in profile mode. Figure 1 illustrates the PSF with a 14.6 m range over different segments of the water column. Only the segment from 1 m-16 m distinguishes itself from the others and then only at angles greater than 80 milliradians. To quantify the similarity of these data sets, the standard deviation was taken at each angle between 10 and 100 milliradians. The average standard deviation for these angles was 12% (8% if the 1 m -16 m set is excluded), thus showing the similarity of the various data sets.

For this cast, 6 good (non-saturated) measurements of the PSF for different ranges exist. These measurements were at ranges of 14.5, 21.8, and 25.4 m with the smaller flashlamp assembly, and 63.7, 47.6, and 87.7 m with the larger flashlamp assembly. These measurements are illustrated in Figure 2. Each measurement was normalized to a different factor of 10 at 1 mrad to illustrate the differences between the data sets. As can be seen there is a general trend of a decrease in slope as the range, and hence scattering length, increases (top to bottom of figure).

To obtain the $D(\theta)$ from these measurements is straight forward in theory, one simply obtains the natural logarithm of the Hankel Transform of the PSF measurements. Unfortunately in working with real data there are two problems which must be overcome. First the data set is not complete in that it does not continue to 180 degrees (or at least in this case to the point where $PSF(\theta) = 0$). Our data stops at 200 milliradians thus one must worry about effects caused by the sudden cutoff of data. This effect causes "ringing" or oscillations to occur in the transform of the longer ranges when significant signal still occurs at 200 milliradians. These oscillations can be reduced by windowing and there is a lot of discussion in the literature on the best choice for a window.⁴ The most effective window in our case proved to be the Hanning window described by the equation:

$$w(\theta) = 0.5 [1 + \cos(\pi \theta / 200)],$$

where θ is in milliradians. Application of this window to the data allows the MTF to be determined with a large reduction in the artificial oscillations and without significant change in the transformed function (however it must be taken into account when the inverse transforms are taken as will be shown later).

The second instrumental effect which must be taken into account is the natural blurring of the PSF caused by the physical size of the source. This effect is a convolution of a high frequency rolloff with the true MTF of the water. This is most easily removed in frequency space where the blur is described by the equation:

$$B(\theta_0, \omega) = 2 J_1(2 \pi \theta_0 \omega) / (2 \pi \theta_0 \omega). \quad (5)$$

J_1 is a first order Bessel function and θ_0 is the angular radius of the source (radius of source divided by range). The dominant effect of this blur is to reduce the high frequency information in the PSF at shorter ranges. In fact for the short range measurement (14.5 m) the MTF of the measurement has no real information above 300 cycles/radian. While the Hanning

function is applied in angular space ("real" space) the effect of the blur function is most easily removed in frequency space(transformed space).

The data reduction process then takes the following steps:

- 1) The data is multiplied by the Hanning window to reduce oscillations in the transform space.
- 2) The Hankel transform:

$$H(\omega, R) = 2 \pi \int_0^{\theta_{max}} J_0(2 \pi \theta \omega) \text{PSF}(\theta, R) \theta \, d\theta, \quad (6)$$

was obtained for each data set.

- 3) The MTF(ω, R) is obtained by dividing the $H(\omega, R)$ by the blur function $B(\theta_0, \omega)$:

$$\text{MTF}(\omega, R) = H(\omega, R) / B(\theta_0, \omega). \quad (7)$$

- 4) The MTF(ω, R) is normalized to 1 at zero frequency. In a complete data set (one that existed from 0 to 180 degrees) for which one did not have to use a windowing function this would remove the effect of the attenuation coefficient from the remaining function. In our case it is an approximation of this process.

- 5) The natural logarithm is taken of the MTF(ω, R) and this is divided by the optical pathlength, $\tau = c R$ (c being the beam attenuation coefficient). Thus the D' function is obtained:

$$D'(\omega) = - \ln(\text{MTF}[\omega, R]) / \tau. \quad (8)$$

The difference between our D' function and the D function of Wells is our normalization to the optical pathlength rather than the range. We do this to increase the applicability of the D' to situations where the water constituents are constant but the concentration (hence c) varies.

Figure 3 illustrates the resultant D' functions. Below 200 mrad there is good agreement between the calculated values. The 14.5 m, 21.8 m, and 63.7 m functions rolloff at higher frequencies. This is the part of the D' that is extremely dependent on the form of the blur function and is probably indicative of a slight error in the range used to generate the function. Over the range from 10 to 100 milliradians the functions were compared using a least squares fit of $D'(87.7 \text{ m})$ to the $D'(R)$. If the D' functions were truly constant than this analysis would point out problems with the measurement of τ (c or R) as a difference in slope and problems in the normalization would show up as a difference in the offset. Table 1 shows the results of these calculations. As can be seen this analysis indicates that there were only small differences in the D' s as evidenced in the slope and offset; on the order of 15% or so.

TABLE 1, Regression of $D'(87.7)$ vs $D'(R)$

Range	slope	offset	r ²
14.5	1.24	-0.06	0.996
21.8	1.14	-0.07	0.993
25.4	1.17	0.062	0.996
61.7	1.13	0.046	0.995
74.6	1.00	0.031	0.997

At this point we investigated how well the $D'(87.7)$ could be used to determine the other PSF's. Figures 4 and 5 illustrate the PSF predicted using the $D'(87.7)$ along with the measured PSF for the best and worst cases. Table 2 illustrates the measured statistics for comparisons between the two PSF's. In all the cases the PSF's have been normalized such that the sum of the PSF from 10 to 100 milliradians was equal to 1. Since the absolute value of the measured PSF was arbitrary this is acceptable.

TABLE 2, Comparison of measured and predicted PSF

Range	average % diff.	average % diff	max % diff
14.5	8.8	18	95
21.8	5.7	11	38
25.4	3.1	32**	70**
61.7	0.15	4.1	13
74.6	-1.0	2.9	13
87.7	0.3	2.1	8.3
Average	3.2	12	39

** (Oscillations in the prediction cause this large error)

This illustrates that the theories of Wells, and hence the small angle theory, works well even at long ranges. We have tried using the D'(87.7) generated here to predict other PSF's from other casts from the same cruise unsuccessfully. If another PSF from the desired cast is used to obtain a new D' the error is reduced to the same order as the above examples. Thus while the PSF can be estimated for various ranges given a single measurement, it is variable and even in the above situation of very clear water, must be measured on the desired day and in the desired water column if it must be known accurately. In situations for which the water is not homogeneous it is even more complicated. We will be looking into situations such as this with other more appropriate data sets and hope to resolve this issue in the near future.

Acknowledgements

I would like to thank Dr. Richard Honey of SRI International for the use of the large flashlamp during the cruise. This work was supported in part by the Applied Physics Laboratory, Johns Hopkins University and by the Ocean Optics Program of ONR (Contract N0014-90-J-1505). I would also like to thank Mr Albert Chapin for his help in collecting the data, and Dr. Howard Gordon for many useful conversations.

References

- 1) Wells, W.H. Theory of small angle scattering. AGARD, No. 61, NATO, 1973, pp. 3.3-1 - 3.3-19.
- 2) Mertens, L. A. and F. S. Replogle, Jr.. Use of point spread functions for analysis of imaging systems in water. J. Opt. Soc. Am., v.67, no.8, 1977, pp.1105-1117.
- 3) Honey, R. C. Beam spread and point spread functions and their measurement in the ocean. in Ocean Optics VI, v.208, 1979, pp.242-248.
- 4) Bracewell, R. N. The Fourier Transform and its applications. pg 250. McGraw-Hill, New York (1978).
- 5) Voss, K. J. and A.L. Chapin. Measurement of the point spread function in the ocean. Appl. Opt. v. 29, no. 25, 1990, pp. 3638-3642.
- 6) Borrowed from Dr. Richard Honey at SRI, Menlo Park, Ca.

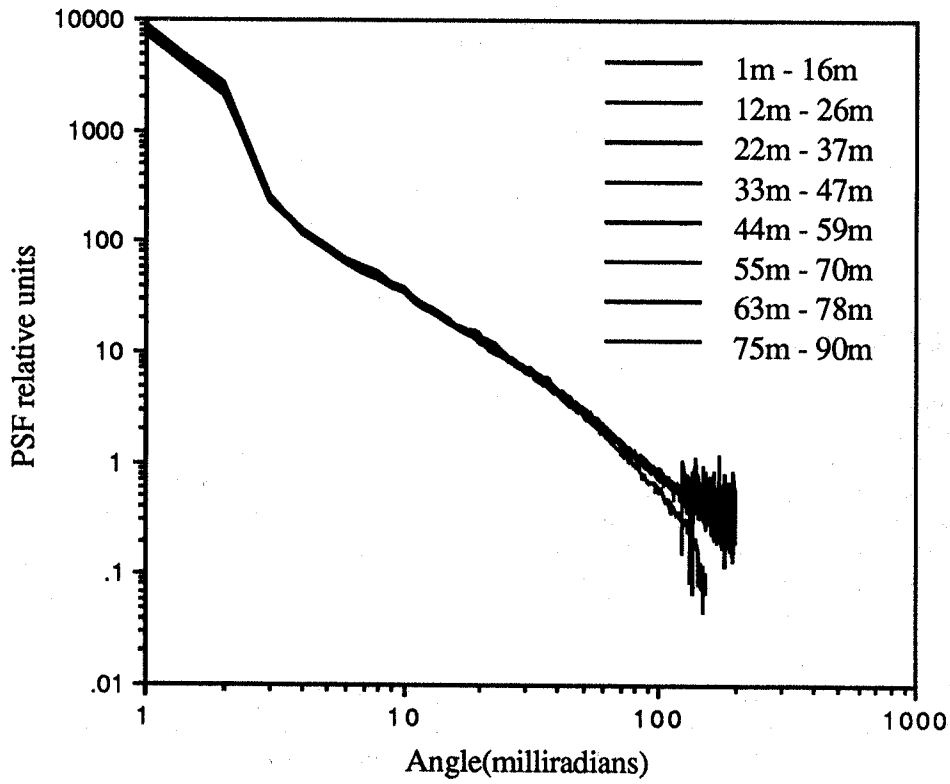


Figure 1

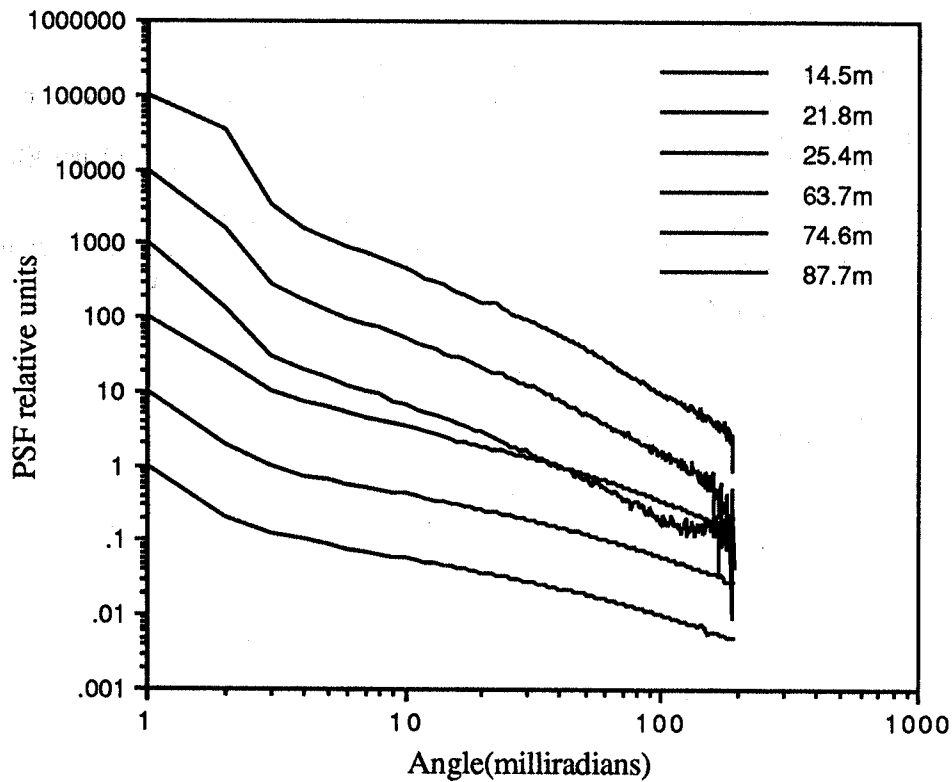


Figure 2

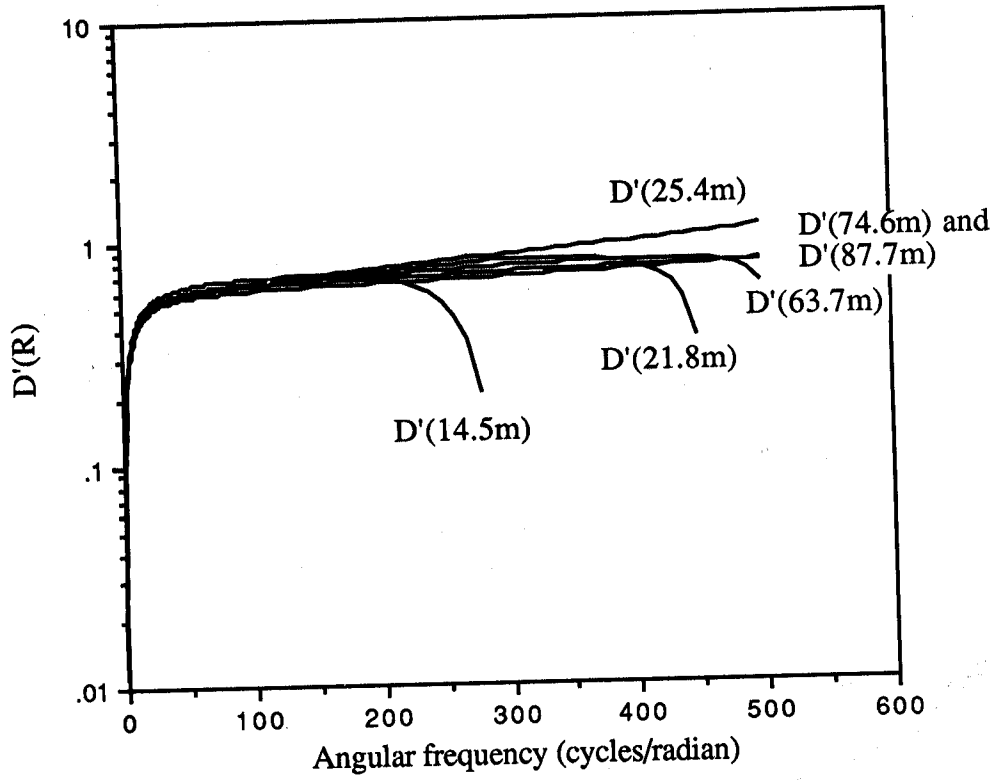


Figure 3

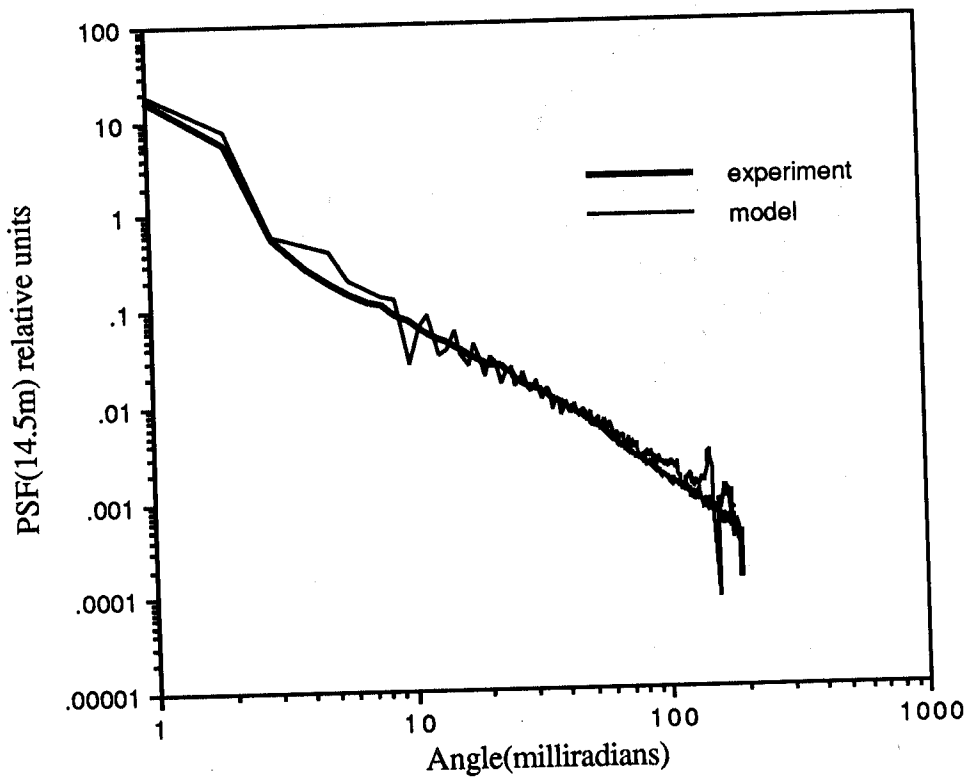


Figure 4

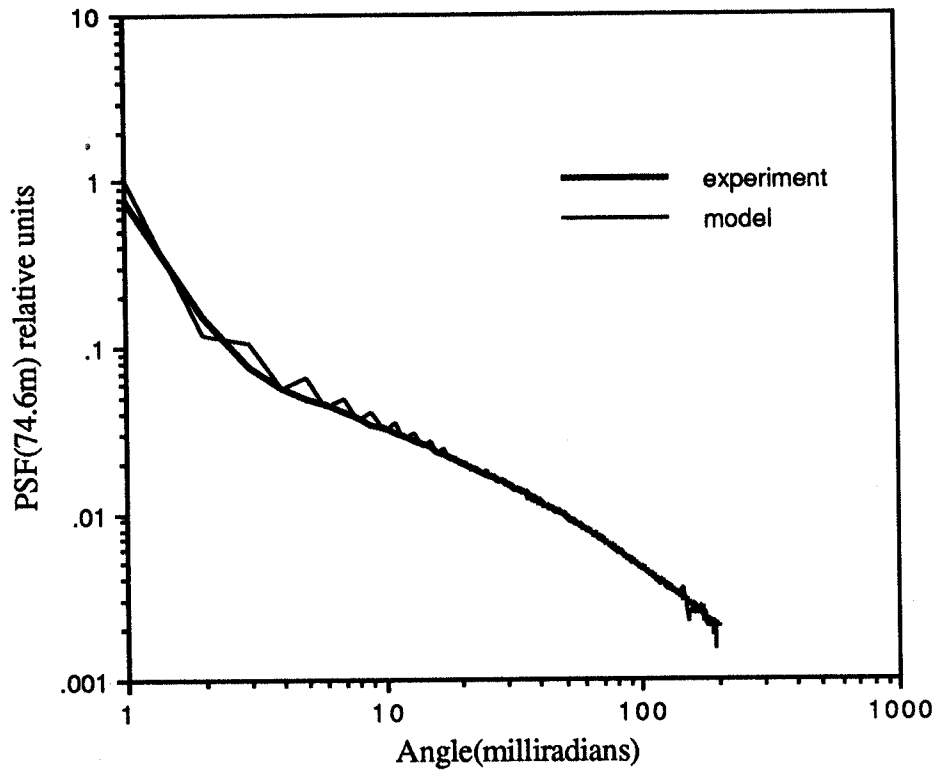


Figure 5